



ELSEVIER

Catalysis Today 48 (1999) 329–336



Magnetic catalyst bodies¹

Wendy Teunissen*, Ageeth A. Bol, John W. Geus

Department of Inorganic Chemistry, Debye Institute, Utrecht University, PO Box 80083, 3508 TB Utrecht, Netherlands

Abstract

After a discussion about the importance of the size of the catalyst bodies with reactions in the liquid-phase with a suspended catalyst, the possibilities of magnetic separation are dealt with. Deficiencies of the usual ferromagnetic particles are the reactivity and the clustering of the particles. A procedure to produce more suitable magnetic particles is to deposit a nickel–iron precursor on a support and to obtain small metal particles by reduction. Subsequently the metal particles are encapsulated in layers of graphitic carbon by exposure to methane at 700°C. Exposure to methane at lower temperature leads to growth of carbon fibrils, which can be controlled by raising the temperature. The alumina support is dissolved in hydrochloric acid. The magnetic properties of nickel–iron alloys prevent clustering of the ferromagnetic particles. © 1999 Elsevier Science B.V. All rights reserved.

Keywords: Nickel-iron alloys; Magnetic properties; Carbon; Encapsulated particles

1. Introduction

In liquids diffusion coefficients are about a factor of 10^4 lower than in gases. Consequently transport limitations are much more likely to be present in liquid-phase reactions. With solid catalysts suspended within liquids the transport within the liquid to the catalyst bodies as well as the transport within porous catalyst bodies can be rate limiting. Especially with reactions in which one or more dissolved species have to react with a gaseous compounds of a limited solubility, transport through the liquid to the catalyst bodies (“external transport”) can limit the rate of the catalytic reaction.

To deal with the transport within the liquid to a suspended catalyst, the catalyst bodies can be assumed to be present in a stagnant liquid. Then the rate of

transport to the catalyst bodies is proportional to $1/D$, where D is the diameter of the catalyst bodies. Since with a fixed weight fraction of catalyst the number of suspended catalyst bodies of diameter D is proportional to $1/D^3$ and the external surface area per catalyst body to D^2 , the total external surface area is proportional to $1/D$. The resulting transport rate to the surface of the catalyst bodies is, hence, proportional to $1/D^2$. To raise the rate of the reaction it is therefore attractive to utilize small catalyst bodies. Also the transport within porous catalyst bodies depends strongly on the size of the bodies. As a result both the activity and the selectivity of suspended catalyst can benefit much from the use of small catalyst bodies.

However, separation of the solid catalyst from the reaction products by filtration or centrifugation calls for a size of the catalyst bodies of at least about 3 μm . Smaller bodies are difficult to separate. The catalyst bodies also have to exhibit a sufficiently high mechanical strength to avoid attrition during the usual vigor-

*Corresponding author.

¹Netherlands institute for Research in Catalysis (NIOK) publication #UU 98-1-06.

ous agitation of the slurry during the catalytic reaction. Small catalyst particles generated by attrition cannot be readily separated from the reaction products.

It is interesting to consider a procedure to separate the solid catalyst from the reaction products that differs from the above conventional centrifugation or filtration, viz., magnetic separation. Magnetic separation asks for sufficiently strong magnetic bodies, which can be achieved most easily by using ferromagnetic bodies. There are, however, two difficulties with the utilization of magnetic bodies as catalyst supports in liquid-phase reactions, viz., the magnetostatic attraction between ferromagnetic particles and the chemical reactivity of most ferromagnetic materials. It is interesting to note that Haque et al. [1] succeeded in separating α - Fe_2O_3 particles of 65 nm out of an aqueous suspension. The magnetization of hematite, α - Fe_2O_3 , is very small. Nevertheless magnetic separation turned out to be possible.

Ferromagnetic particles usually exhibit a permanent magnetic moment and thus a mutual attraction leading to clustering of magnetic particles. Clustering of ferromagnetic particles can be prevented by using soft ferromagnetic materials, in which the remanent magnetic moment (the magnetic moment in the absence of a magnetic field) is low. Soft magnetic materials are usually produced from nickel–iron alloys. Alternatively the magnetic interaction between magnetic bodies can be decreased by the application of “spacers” on the magnetic particles, species that keeps the ferromagnetic particles at a relatively large mutual distance. The state of the art as used with ferrofluids is to apply polymer molecules on the surface of the ferromagnetic particles.

Strong ferromagnetic particles consist of metallic iron or iron alloys. Though the magnetic properties of metallic ferromagnetics are attractive, it is obvious that the chemical reactivity is high. It is furthermore difficult to produce metallic particles of a size substantially less than 1 μm . Alternatively ferrimagnetic particles can be used, such as, magnetite (Fe_3O_4). The state of the art usually involves application of small magnetite bodies. However, magnetite is also fairly reactive, especially with acid, but also with complexing agents that are often encountered with liquid-phase catalytic reaction.

To remedy the above deficiencies of the usual magnetic materials, we developed a procedure in

which we can easily produce small ferromagnetic metal particles. The procedure was furthermore extended to provide inert ferromagnetic metal particles. Small ferromagnetic particles are produced by application of a suitable precursor onto a support that can be dissolved in an acid or alkaline liquid. Since it is a common practice to prevent sintering of small metal particles by the application of a support, the production of (very) small metal particles can be achieved readily. Subsequently we encapsulate the ferromagnetic metal particles resulting from the reduction at elevated temperatures in a gas flow by graphitic carbon layers. When it is desired to use “spacers” to keep the ferromagnetic particles separated, we grow carbon filaments of a limited length out of the metal particles before encapsulating the metal particles. Finally we can dissolve the support without affecting the ferromagnetic metal particles that are protected by the carbon layers.

To produce soft magnetic particles, which consist preferably of nickel and iron, we have employed deposition–precipitation of complex cyanides, in which nickel and iron are mixed on a molecular level. Different complex cyanides are used to arrive at different nickel-to-iron ratios as the initial support alumina has been used. After calcination of the complex cyanides to produce the corresponding mixed oxides, the supported oxides are reduced in a flow of hydrogen. Subsequently encapsulation is performed in a flow of methane. The support is next dissolved in hydrochloric acid to provide the small encapsulated ferromagnetic particles.

The catalytic properties of the above ferromagnetic supports have been evaluated by the hydrogen reduction of nitrobenzene to aniline. Palladium is applied on the carbon encapsulating the ferromagnetic particles, after which the reduction of nitrobenzene is performed at room temperature.

2. Experimental

2.1. Preparation of encapsulated nickel–iron particles

To prepare alumina-supported nickel–iron alloy particles deposition-precipitation of complex cyanides was performed [2]. To obtain different nickel-to-iron

ratios the iron containing precursors were potassium ferrocyanide trihydrate, ammonium ferrocyanide hydrate, potassium ferricyanide and sodium nitroferrocyanide dihydrate. When no potassium is included in the precipitated complex cyanides, the nickel-to-iron ratio resulting from the above cyanides is 2:1, 2:1, 1.5:1, and 1:1, respectively.

The aqueous iron cyanide solutions were injected into a vigorously stirred suspension of alumina in an aqueous solution of nickel nitrate at a rate of 1 ml/min. The pH of the suspension had previously been acidified to 5. After completion of the injection, the loaded support was filtered, washed and dried. A sieve fraction of 425–850 μm was calcined in a flow of 20% oxygen in He (95 ml/min) at 300°C for 3 h.

A weighed sample of the thus calcined material containing an alumina-supported nickel–iron mixed oxide (about 20 wt% of iron–nickel alloy) was placed in a specially designed reactor and reduced in a flow of 20% hydrogen in argon (flow rate 100 ml/min). The temperature was raised to 700°C within 2 h and kept at this level for 2 h.

Encapsulation of the metal particles in graphitic layers was executed at different temperatures. After the above reduction the reactor was cooled to the desired temperature under hydrogen. Next a flow of 20% methane (balance argon, total flow rate 100 ml/min) was passed through the reactor. The conversion of methane to hydrogen and deposited carbon was assessed by recording the composition of the gas flowing out of the reactor gaschromatographically. After completion of the encapsulation the sample was cooled to room temperature in a flow of argon. The alumina was finally dissolved by boiling the sample in nitric or hydrochloric acid.

2.2. *Application of palladium on magnetic carbon bodies and testing of catalytic activity*

To enhance the reactivity of the carbon surface of the encapsulated iron–nickel particles, the material resulting from the dissolution of the alumina within hydrochloric acid was kept in refluxing 65% nitric acid for 10 min. This treatment leads to carboxylic surface groups that are able to bind the amine complex of palladium. After thorough washing, the encapsulated magnetic particles were suspended in water under a nitrogen atmosphere, which was maintained

during the next step of the procedure, and the pH was installed at a level of 5. Subsequently an aqueous solution of $\text{Pd}(\text{NH}_3)_4(\text{NO}_3)_2$ was injected into the suspension under vigorous stirring. The solid was filtered and dried for 16 h in a nitrogen flow at 80°C.

Before suspension in the liquid for the hydrogenation, a weighed amount of the catalyst was prereduced in a separate vessel in a flow of hydrogen. The temperature was linearly increased with 1.9 K/min to 250°C. Next the catalyst was exposed to air and brought into 125 ml isopropylalcohol contained in a double-walled reaction vessel of 150 ml. Circulating thermostated water through the wall of the vessel carefully controlled the temperature of the reactor. Four large stirrer blades attached to a shaft mounted centrally in the vessel and connected to a gas recirculation device vigorously agitated the liquid. In order to expel air from the vessel a flow of hydrogen was passed through the liquid for 2 h. Next 6.5 ml of nitrobenzene was injected into the liquid, mixed within the alcohol and the consumption of hydrogen was recorded [3].

2.3. *Characterization of the materials and the catalysts*

A Perkin-Elmer Optima-3000 was used to establish the chemical composition of the calcined cyanide precursors by inductively coupled plasma (ICP) analysis. To assess the reaction to a mixed oxide during calcination and to alloy particles with graphite X-ray diffraction (XRD) was performed. XRD patterns were recorded at room temperature with a Nonius PDS 120 powder diffractometer system equipped with a position-sensitive detector with a range of 2θ of 120°. The radiation used was $\text{Co } K_{\alpha_1}$ ($\lambda=1.78897 \text{ \AA}$).

For further characterization the catalysts were examined in a Philips EM-420 transmission electron microscope (TEM) operated at an accelerating voltage of 120 kV. The chemical composition of the encapsulated alloy particles was determined using a Philips CM-200 FEG electron microscope operated at 200 kV. The microscope was equipped with a field-emission gun and an EDX facility for elemental analysis of a spot size of 4 nm^2 . Samples were prepared by suspending the solid in ethanol under ultrasonic vibration. One or two drops of the thus prepared suspension were brought onto a holed carbon film on a copper grid.

Magnetic measurements were performed using a vibrating sample magnetometer (VSM), which consisted of an electromagnet (maximum field strength 12 kOe) with a sample cell holder vibrating between the pole faces. Four coils measured the magnetization; the coils were situated within the magnet two on each side of the sample cell. The AC voltage induced in the coils was transduced to a DC voltage and fed to a “lock-in” amplifier. The equipment was calibrated using bulk nickel standards. The magnetic measurements were performed at room temperature.

3. Results and discussion

3.1. Preparation of encapsulated nickel–iron particles

ICP–AES measurements provided information about the nickel-to-iron ratio of the calcined nickel–iron cyanide complexes on alumina. Incorporation of potassium, when potassium salts of ferro- or ferricyanide were used, was also established. The results, represented in Table 1, show that the intended nickel-to-iron ratio was only obtained when the sodium salt of nitroferricyanide complex was used. With potassium ferrocyanides and to a smaller extent with the potassium ferricyanide, the nickel-to-iron ratios were lower. The lower nickel-to-iron ratio point to precipitation of $K_2NiFe(CN)_6$ or $(NH_4)_2NiFe(CN)_6$. Also the experimentally observed lower loading of nickel and iron oxide indicate precipitation of potassium containing compounds. The calculated loading, based on the intended amount of the oxides of nickel and iron, amounts to 18.8 wt%. The loading of the alumina from potassium ferrocyanide with nickel–iron oxide and potassium oxide is 18.9 wt%, while that of the alumina from potassium ferricyanide is

18.6 wt%, which agrees with the precipitation of $K_2NiFe(CN)_6$, and with the precipitation of a smaller amount of $KNiFe(CN)_6$. With the precipitation of $(NH_4)_2NiFe(CN)_6$ the eventual total loading is smaller, since the ammonium volatilizes during the calcination.

XRD measurements on the calcined alumina-supported cyanide precursors showed reaction to $NiFe_2O_4$ together with NiO, which was to be expected from the nickel-to-iron ratios, which are higher than 0.5. Diffraction maxima due to either Fe_2O_3 or other iron oxides or potassium compounds were not observed.

To produce encapsulated nickel–iron particles, the supported oxides were reduced in situ after which the loaded supports were exposed to methane at different temperatures. To assess the effect of the nickel-to-iron ratio on the saturation magnetization, the magnetization was measured before encapsulation. It is well known that the saturation magnetization of nickel–iron alloys depends upon the nickel-to-iron ratio. Table 2 shows the experimentally measured saturation magnetization of the alumina-supported nickel–iron particles. With bulk nickel–iron alloys, the alloy of a nickel-to-iron ratio of 1.0 exhibits a saturation magnetization of $156 \text{ G cm}^3/\text{g}$ and the alloy with a nickel-to-iron ratio of 3.7 of $10^4 \text{ G cm}^3/\text{g}$. Interpolation predicts a saturation magnetization of about $130 \text{ G cm}^3/\text{g}$ for an alloy with a nickel-to-iron ratio of 1.75 and of

Table 2
The saturation magnetization of the prepared nickel–iron alloy particles on alumina

Ni:Fe ratio of sample (wt% K)	Msat ($\text{G cm}^3/\text{g}$)
1.72:1.00 (4.27)	7.5
1.48:1.00 (0)	59.6
1.57:1.00 (0.38)	63.7
1.00:1.00 (0)	97.8

Table 1
Results of ICP–AES analysis of calcined nickel–iron cyanide complexes on alumina

Adjusted			Measured			
Precursor 1	Precursor 2	Ni:Fe ratio	Ni:Fe ratio	Metal loading (wt%)	K (wt%)	Na (wt%)
$Ni(NO_3)_2$	$K_4Fe(CN)_6$	2:1	1.72:1.00	14.6	4.27	–
$Ni(NO_3)_2$	$(NH_4)_4Fe(CN)_6$	2:1	1.48:1.00	14.9	–	–
$Ni(NO_3)_2$	$K_3Fe(CN)_6$	1.5:1	1.57:1.00	18.2	0.38	–
$Ni(NO_3)_2$	$Na_2Fe(CN)_5NO$	1:1	1.00:1.00	18.8	–	0

about $140 \text{ G cm}^3/\text{g}$ with a nickel-to-iron ratio of 1.5. The experimental saturation magnetization being lower than the values measured on bulk alloys can be due to an incomplete reduction or to oxidation during transfer in the aluminum vessel on which the measurement was performed, though the transfer was done in a nitrogen atmosphere. Whereas the other nickel-iron alloys display a saturation magnetization decreasing with an increasing nickel content, that of the alloy with a nickel-to-iron ratio of 1.72 shows a higher saturation magnetization. This may point to separate precipitation of species containing only nickel besides the above $\text{K}_2\text{NiFe}(\text{CN})_6$. Reduction leads to an alloy of a nickel-to-iron ratio of 1.0 and nickel particles, which are more readily completely reduced and less liable to oxidation.

To study the encapsulation of the supported alloy particles, a methane flow was passed over the previously reduced materials for 60 min. A gas chromatograph measured the composition of gas flow exiting

the reactor. At a reaction temperature of 700°C the methane consumption was 2 ml/min during the first 10 min. Subsequently the alloy particles deactivated and the methane consumption dropped to less than 0.1 ml/min. At lower reaction temperatures up to 10 ml/min reacted to carbon and hydrogen, while the deactivation was much less. The high rate of methane consumption indicated the growth of carbon fibers, which was confirmed by TEM images. Fig. 1 shows a TEM image of a catalyst of a nickel-to-iron ratio of 1.0 after exposure to methane at 530°C during 60 min. The formation of carbon fibrils at 530°C is apparent from this figure, whereas merely encapsulation proceeded at 700°C .

Within the nickel-to-iron range studied here, the encapsulation of the alloy particles and the growth of carbon fibrils do not depend on the nickel-to-iron ratio. However, the presence of potassium within the materials strongly affected the encapsulation as well as the growth of carbon fibrils. The material of a nickel-to-

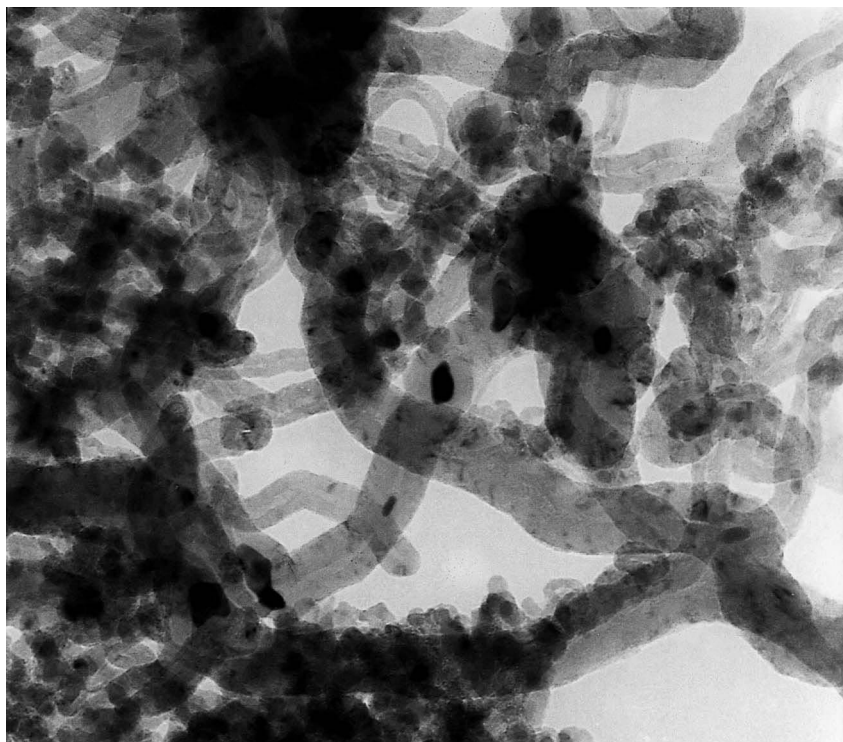


Fig. 1. TEM micrograph of carbon fibrils formed after passing over methane at a temperature of 530°C . The nickel-to-iron ratio of the metal particles is 1.00 (1 cm=40 nm).

iron ratio of 1.72 containing 4.27 wt% potassium did not exhibit decomposition of methane irrespective of the reaction temperature. Neither encapsulation nor growth of carbon fibrils proceeded. The behavior of the material with 0.38 wt% potassium, on the other hand, did not deviate from that of the materials without potassium.

XRD patterns were taken of the alumina-supported encapsulated alloy particles. The diffraction patterns show that the nickel–iron alloy in particles encapsulated at 700°C remained present and the presence of graphite.

For the application as a ferromagnetic support, the magnetic properties of the encapsulated alloy particles are decisive. Fig. 2 shows the magnetization as a function of the field strength of alumina supported alloy particles of a nickel-to-iron ratio of 1.0 after reduction and encapsulation. It can be seen that the magnetization after encapsulation is even higher than that after reduction only. The increase in magnetization during encapsulation is due to an increase in the extent of reduction. As to be expected keeping the supported mixed oxide particles in a flow of hydrogen at 700°C is not sufficient to bring about complete reduction. Reaction with methane led to further reduction and thus to a higher saturation magnetization. Since the magnetization dropped to zero when the magnetic field was switched off and, hence, displayed

no remanence, the ferromagnetic particles are magnetically soft.

To release the encapsulated alloy particles, the alumina support was removed by treatment with boiling hydrochloric or nitric acid. Nitric acid appeared to oxidize the carbon layers too strongly. A treatment for 2 h with boiling nitric acid left almost no solid material. The removal of magnetic material was indicated by a drop of the saturation magnetization from 108 to 17 G cm³/g. A treatment with boiling hydrochloric acid, on the other hand, released the encapsulated alloy particles. As indicated by magnetic measurements, all particles that are not completely encapsulated are removed during the first 30 min. Boiling for 8 h completely dissolved the alumina and left the encapsulated alloy particles. The complete removal of the alumina was confirmed by XRD, TEM and magnetic measurements. Fig. 3 shows an electron micrograph of the released encapsulated particles. The saturation magnetization of the remaining solid was 88 G cm³/g, which was sufficiently high to allow one to separate the small particles rapidly by an inhomogeneous magnetic field.

3.2. Application of palladium and testing of the resulting magnetically supported catalyst

To provide a larger carbon surface area per unit weight of catalyst a material was utilized in which

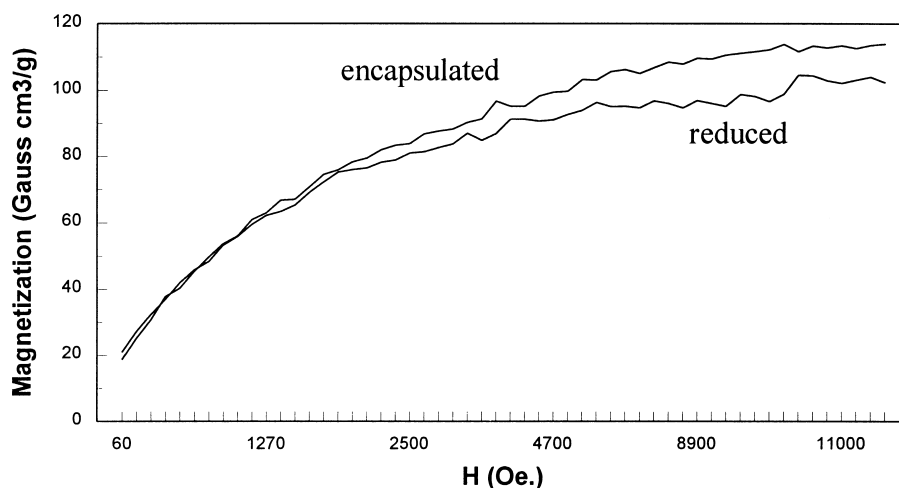


Fig. 2. VSM measurements of alloy particles with nickel-to-iron ratio of 1.00 on alumina, after reduction and after encapsulation with methane at 700°C.

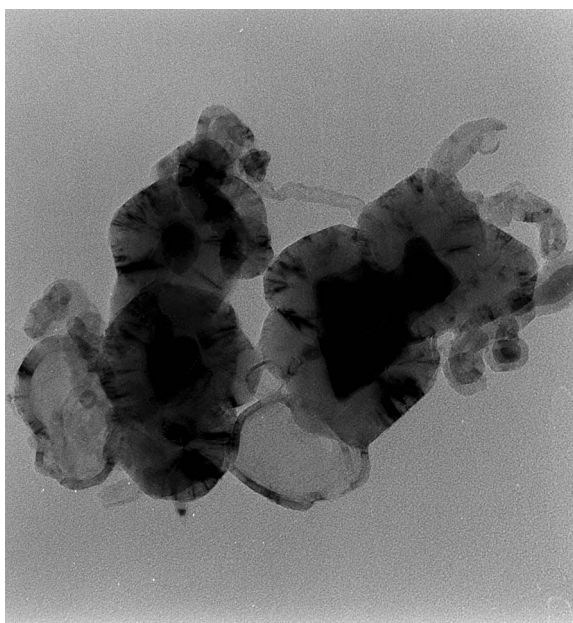


Fig. 3. TEM micrograph of isolated encapsulated nickel–iron alloy particles (1 cm=25 nm).

carbon fibrils had grown out of the alloy particles before the particles had been encapsulated. The BET surface area of the magnetic carbon support used was 75 m²/g. The consumption of hydrogen measured

during a temperature-programmed reduction experiment pointed to a palladium content of about 0.1 wt%. The saturation magnetization of the catalyst after application of the palladium and reduction of the palladium had decreased to 65 G cm³/g. The drop in saturation magnetization is presumably to the short pretreatment with nitric acid that removed the carbon layers around some of the alloy particles.

The loaded magnetic support was extensively studied in the Philips CM-200 electron microscope. Fig. 4 shows an image taken with secondary electrons that show the external shape of the bodies present within the materials. Strongly intertwined carbon fibrils of a circular cross-section are apparent. Fig. 5 represents a transmission electron micrograph of the electron scattered over a large angle. The dark-field image was taken with a ring detector. The scattering over large angles of electrons passing through a specimen strongly depends upon the nuclear charge of the atoms present in the specimen. Heavy elements are scattering electron much more than light elements. The alloy particles are hence clearly indicated in Fig. 5. It can easily be seen that the alloy particles are present encapsulated by carbon, which scatters electron much less than iron and nickel.

The individual alloy particles were analyzed by energy-dispersive X-ray analysis (EDX). The particles

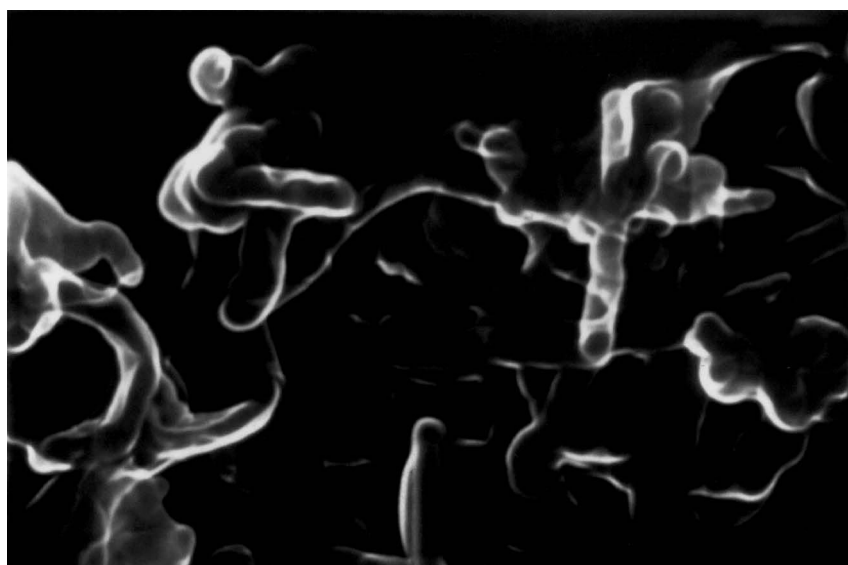


Fig. 4. SEM micrograph of a network of carbon fibrils used to prepare a palladium catalyst (1 cm=50 nm).



Fig. 5. Dark field STEM micrograph using a ring detector of the carbon fibril network used to prepare a palladium catalyst. The enlightened particles are nickel–iron alloy particles. The nickel-to-iron ratio in these particles is 1.0, as detected with EDX analysis (1 cm=50 nm).

exhibited uniformly and fairly accurately a nickel-to-iron ratio of 1.0, thus confirming the analytical data.

The hydrogen consumption during the hydrogenation of nitrobenzene at 25°C was 1.5 ml/min, which is reasonable, considering the low loading of the support. Separation of the very small clusters of carbon fibrils could be performed very easily by means of an inhomogeneous magnetic field.

4. Conclusions

Deposition precipitation of $\text{NiFe}(\text{CN})_5\text{NO}$ provides small alumina supported nickel–iron particles upon reduction with a nickel-to-iron ratio of 1.00. Exposure to methane at 700°C leads to graphite encapsulated alloy particles, while at lower temperatures the growth of carbon fibrils take place. The alumina support is dissolved in hydrochloric acid. The magnetic properties of the nickel–iron alloy prevent clustering of the

ferromagnetic particles with redispersion. The application of the palladium supported magnetic catalyst bodies in the hydrogenation of nitrobenzene indicated that the magnetic catalyst bodies are suitable as support material, but the preparation procedure needs to be optimized.

References

- [1] M.F. Haque, R. Aidun, C. Moyer, S. Arajs, *J. Appl. Phys.* 63 (1988) 3239.
- [2] E. Boellaard, A.M. van der Kraan, J.W. Geus, in: *Proceedings of the Conference On the Scientific Bases for the Preparation of Heterogeneous Catalysts*, Louvain-la-Neuve, Belgium, 1995.
- [3] M.S. Hoogenraad, R.A.G.M.M. van Leeuwarden, G.J.B. van Breda Vriesman, A. Broersma, A.J. van Dillen, J.W. Geus, in: *Proceedings of the Conference On the Scientific Bases for the Preparation of Heterogeneous Catalysts*, Louvain-la-Neuve, Belgium, 1995.